Hematopoietic NLRP3 and AIM2 inflammasomes promote diabetes-accelerated atherosclerosis, but increased necrosis is independent of pyroptosis

Cheng-Chieh Hsu, Trevor P. Fidler, Jenny E. Kanter, Vishal Kothari, Farah Kramer, Jingjing Tang, Alan R. Tall, Karin E. Bornfeldt

Supplemental Materials

Supplemental Tables: 8
Supplemental Data Figures: 11
Original immunoblots and unmarked lesion images are shown in Supplemental Figures 12-14.

Supplemental Table 1: Information on assays or kits used for measuring plasma analytes.

Assay/kit	Manufacturer	Catalog number
Mouse IL-1β ELISA kit	Thermo Fisher Scientific	88-7013-88
Mouse IL-18 ELISA kit	Thermo Fisher Scientific	88-50618-88
Mouse APOC3 ELISA kit	Abcam	ab217777
Cholesterol E Assay	Wako Diagnostics	999-02601
Triglyceride Liquicolor	Stanbio Laboratory	2100-430
Cholesterol Liquicolor	Stanbio Laboratory	1010-430
Mouse Enhanced Sensitivity Master Buffer Kit	BD Biosciences	562246
Mouse IL-1β Enhanced Sensitivity Flex Set	BD Biosciences	562278

Supplemental Table 2: Information on antibodies and reagents used for immunofluorescence.

Antibody/reagents	Catalog number	Manufacturer	Concentration/dilution
Mac-2	CL8942AP	Cedarlane	2 μg/mL
α-Smooth muscle actin	AB5694	Abcam	0.4 μg/mL
APOC3	-	Ionis Pharmaceuticals	1:1000
APOB-biotinylated	BAF3556	Novus Biologicals	4 μg/mL
APOE	AB183597	Abcam	0.35 μg/mL
Biotinylated Goat IgG control	BAF108	Novus Biologicals	See APOB
Rabbit IgG control	02-6102	Thermo Fisher Scientific	See APOE, α-SMA
Rat IgG control	553927	BD Biosciences	See Mac-2
Anti-rabbit IgG, AlexaFluor647	A21245	Thermo Fisher Scientific	1:500
Anti-rat IgG, AlexaFluor555	405420	BioLegend	1:500
Tyramide-AlexaFluor488	B40953	Thermo Fisher Scientific	Per manufacturer's instructions
HRP-conjugated Streptavidin	016-030-084	Jackson ImmunoResearch Labs	1:5000
Mounting Medium with DAPI	H-2000	Vector Laboratories	Per manufacturer's instructions
Avidin/Biotin Blocking Kit	SP-2001	Vector Laboratories	Per manufacturer's instructions

Supplemental Table 3: Circulating leukocyte counts from a 4-week type 1 diabetes mouse model.

(k/μL)	Non-diabetes	Diabetes	Virus control
Total leukocytes	5.98 ± 0.314	4.78 ± 0.596	7.21 ± 0.483†
Monocytes	0.355±0.031	0.143±0.018***	0.351±0.04††
GR1^{high} (Ly6C^{high}) Monocytes	0.215±0.020	0.101±0.017***	0.207±0.021†
GR1^{low} (Ly6C^{low}) Monocytes	0.102±0.013	0.032±0.004***	0.127±0.02†††
Neutrophils	0.968±0.062	2.01±0.327*	0.357±0.040†††‡‡

Female low-density lipoprotein receptor-deficient mice with a virus glycoprotein transgene (*Ldlr*$^{-/-}$*;Gp*^{Tg}) were rendered diabetic with lymphocytic choriomeningitis virus (LCMV). Saline was used as a control. *Ldlr*$^{-/-}$ mice without the glycoprotein (*Ldlr*$^{-/-}$*;Gp*^{0}) transgene were injected with LCMV as a virus control. At the onset of diabetes, the animals were switched to a low-fat, semipurified diet with no added cholesterol (LFD) and maintained for 4 weeks. Mice were bled retro-orbitally under isoflurane sudation after 4 weeks of diabetes. The total leukocyte count was determined by a hematology analyzer (Drew Scientific). Erythrocytes were lysed and removed with an ammonium-chloride-potassium buffer before staining. The leukocytes were stained for viability, CD45, CD115, and GR1. The single cell, live, CD45+, CD115+ population was identified as monocytes. The monocyte population was divided into GR1^{high} (Ly6C^{high}) and GR1^{low} (Ly6C^{low}) subpopulations. The single cell, live, CD45+, CD115-, and GR1^{high} population was identified as neutrophils. The single cell, live, CD45+ population was identified as leukocytes and normalized to the total leukocyte count. Flow analysis was conducted on a FACSCanto RUO Flow cytometer (BD Biosciences). Data show means ± SEM (n=21, 19, 7 mice/group). Statistical analyses were performed by Kruskal-Wallis test and Dunn's multiple comparisons tests. Normality test was performed by D'Agostino & Pearson test. *Significant between non-diabetes and diabetes groups. †Significant between diabetes and virus control groups. ‡Significant between non-diabetes and virus control groups. P<0.05 (*, †, ‡), <0.01 (**, ††, ‡‡), and < 0.001 (***, †††, ‡‡‡) are considered statistically significant. Outliers were removed based on Grubbs' test with alpha = 0.01. (0,1,0) data points were removed for monocytes; (0,1,0) data points were removed for GR1^{high} (Ly6C^{high}) monocytes; no other data points were removed.

Supplemental Table 4: Information on antibodies used for flow cytometer analysis.

Antibody	Clone/catalog number	Manufacturer
CD45-FITC	30-F11	eBioscience
CD115-APC	AFS98	eBioscience
GR1-PE-Cy7	RB6-8C5	eBioscience
Viability dye e450	65-0863-14	eBioscience

Supplemental Table 5: Information on antibodies and reagents used for immunoblotting and genotyping.

Antibody/reagent	Catalog number	Manufacturer	Concentration/dilution
Gasdermin D	-	Genentech	1 μg/mL
Caspase-1	14-9832-37	Thermo Fisher Scientific	1:50
Anti-rat HRP	A9037	Sigma-Aldrich	1:1000
Mouse F4/80 positive selection kit	8802-6863-74	Thermo Fisher Scientific	Per manufacturer's instructions
Ultrapure mouse CD11B microbeads	130-126-725	Miltenyi Biotec	Per manufacturer's instructions
DNA isolation and purification kit	158043	QIAGEN	Per manufacturer's instructions
RIPA lysis and extraction buffer	89900	Thermo Fisher Scientific	Per manufacturer's instructions
Protease and phosphatase inhibitor cocktail	78440	Thermo Fisher Scientific	Per manufacturer's instructions

Supplemental Table 6: Circulating leukocyte counts from a 4-week diabetes mouse model with and without hematopoietic GSDMD-deficiency.

(k/μL)	No diabetes (*Gsdmd*$^{+/+}$)	No diabetes (*Gsdmd*$^{-/-}$)	Diabetes (*Gsdmd*$^{+/+}$)	Diabetes (*Gsdmd*$^{-/-}$)
Total leukocytes	10.7±0.79	9.94±0.79	7.72±1.15*	7.59±0.794
Monocytes	0.786±0.06	0.714±0.05	0.346±0.05***	0.327±0.04‡‡‡
GR1^{high}(Ly6C^{high}) Monocytes	0.576±0.06	0.466±0.03	0.227±0.04***	0.222±0.03‡‡‡
GR1^{low} (Ly6C^{low}) Monocytes	0.206±0.02	0.199±0.02	0.083±0.01***	0.074±0.01‡‡‡
Neutrophils	1.85±0.22	1.69±0.17	1.56±0.21	1.75±0.19

Female *Ldlr*$^{-/-}$*;Gp*^{Tg} mice were maintained on a high-fat diet (HFD) for 12 weeks to allow the formation of pre-existing lesions. Mice were lethally irradiated and received bone-marrow cells from animals with and without gasdermin D-deficiency. The animals were maintained on a chow diet and recovered for 5 weeks. Mice were rendered diabetic (D) with lymphocytic choriomeningitis virus (LCMV). Saline was used as a control (non-diabetic, ND). At the onset of diabetes, the animals were switched to a low-fat, semipurified diet with no added cholesterol (LFD) and were maintained for 4 weeks. Total leukocytes were measured with a hematology analyzer and the cell types were identified by flow cytometry as described in Supplemental Table 3. Data show means ± SEM (n=22, 25, 24, 22 mice/group). Statistical analyses were performed by Kruskal-Wallis test and Dunn's multiple comparisons tests. Normality test was performed by D'Agostino & Pearson test. *Significant between non-diabetes (WT) and diabetes (WT) groups. †Significant between non-diabetes (WT) and non-diabetes (KO) groups. ‡Significant between non-diabetes (KO) and diabetes (KO) groups. P<0.05 (*, †, ‡), <0.01 (**, ††, ‡‡), and < 0.001 (***, †††, ‡‡‡) are considered statistically significant. Outliers were removed based on Grubbs' test with alpha = 0.01. (1,0,0,0) data points were removed for total leukocytes; (1,0,0,0) data points were removed for monocytes; (1,1,1,1) data points were removed for GR1^{low} (Ly6C^{low}) monocytes; (1,0,0,0) data points were removed for neutrophils; no other data points were removed.

Supplemental Table 7: Lesion immunoreactivity area from a 4-week diabetes mouse model with and without hematopoietic GSDMD-deficiency.

x1000 μm²	No diabetes (*Gsdmd*$^{+/+}$)	No diabetes (*Gsdmd*$^{-/-}$)	Diabetes (*Gsdmd*$^{+/+}$)	Diabetes (*Gsdmd*$^{-/-}$)	Diabetes Effect p-value	Genotype Effect p-value
APOB^{+} area	74.5±9.3	73.6±6.7	92.9±8.4	66.8±5.7	0.451	0.0824
APOE^{+} area	146.6±13.1	132.3±10.6	184.8±10.4	142.2±6.8§	0.026	0.0087
APOB^{+} APOE^{+} area	57.0±6.8	53.1±4.9	77.9±5.8*	53.0±4.0§§	0.04	0.0097
MAC2^{+} area	48.5±6.3	42.3±3.9	52.9±3.9	37.9±4.0	0.996	0.0245
αSMA^{+} area	22.5±4.0	25.7±4.7	25.9±5.2	21.0±3.5	0.8845	0.8453
APOC3^{+} area	18.2±3.5	13.4±3.3	27.4±6.0	27.9±7.1	0.026	0.69

Female *Ldlr*$^{-/-}$*;Gp*^{Tg} mice were maintained on a high-fat diet (HFD) for 12 weeks to allow the formation of pre-existing lesions. Mice were lethally irradiated and received bone-marrow cells from animals with and without gasdermin D-deficiency. The animals were maintained on a chow diet and recovered for 5 weeks. Mice were rendered diabetic (D) with lymphocytic choriomeningitis virus (LCMV). Saline was used as a control (non-diabetic, ND). At the onset of diabetes, the animals were switched to a low-fat, semipurified diet with no added cholesterol (LFD) and were maintained for 4 weeks. Aortic sinus immunoreactivity of APOB^{+}, APOE^{+}, APOB^{+}APOE^{+}, MAC2^{+}, αSMA^{+}, and APOC3^{+} area was stained and measured. Immunofluorescence staining was conducted at 0 μm. Data show means ± SEM (n=19, 20, 21, 19 mice/group). Statistical analyses were performed by two-way ANOVA followed by Tukey's multiple comparisons test. Normality test was performed by D'Agostino & Pearson test. *Significant between non-diabetes (WT) and diabetes (WT) groups. †Significant between non-diabetes (WT) and non-diabetes (KO) groups. ‡Significant between non-diabetes (KO) and diabetes (KO) groups. §Significant between diabetes (WT) and diabetes (KO). P<0.05 (*, †, ‡, §), <0.01 (**, ††, ‡‡, §§), and < 0.001 (***, †††, ‡‡‡, §§§) are considered statistically significant. p-values between two groups were calculated by multiple comparisons test and the overall group effects (p-values) as calculated by two-way ANOVA. Outliers were removed based on Grubbs' test with alpha = 0.01. (0,0,1,0) data points were removed for APOB^{+}APOE^{+} area; (0,0,1,0) data points were removed for MAC2^{+} area; (0,0,0,1) data points were removed for APOE^{+} area; no other data points were removed.

Supplemental Table 8: Comparison of phenotypes in the LCMV and STZ models of type 1 diabetes. Mean ± SEM (n=7-25 mice/group); statistical analysis by two-tailed unpaired t-test (for normally distributed data) or Kruskal-Wallis (for non-parametric data). Note that the LCMV and STZ *Ldlr*$^{-/-}$ models of diabetes were studied to address different questions and that the studies were not performed side-by-side. The data should therefore be interpreted with caution.

	Diabetic LCMV	**Diabetic STZ**	**p-value**
Blood glucose (mmol/L)	28.2±1.1	21.6±2.6	0.01
Plasma cholesterol (mmol/L)	7.9±0.7	30.6±5.2	<0.0001
Plasma triglycerides (mmol/L)	2.9±0.2	3.0±0.2	0.747
Plasma APOC3 (μg/mL)	229.5±29.2	742.8±209.3	0.0009
Plasma IL-1β (fg/mL)	580.5±235.1	92.0±32.9	0.173
Plasma IL-18 (pg/mL)	397.5±55.3	523.7±150.7	0.337
Sinus lesion area (μm^{2}x1000)	350.7±27.0	319.6±58.0	0.219
Necrotic core area (%)	19.0±1.6	14.9±3.9	0.278
Mac2$^+$ lesion area (%)	16.5±1.7	17.3±4.6	0.847
α-SMA$^+$ lesion area (%)	9.8±2.0	2.3±0.5	0.055
APOB$^+$ lesion area (%)	26.5±1.7	21.8±2.1	0.128
APOE$^+$ lesion area (%)	55.5±3.7	19.6±3.8	<0.0001
APOC3$^+$ lesion area (%)	8.8±1.1	31.7±1.6	<0.0001
Lesion severity score	9.0±0.3	9.7±0.9	0.504

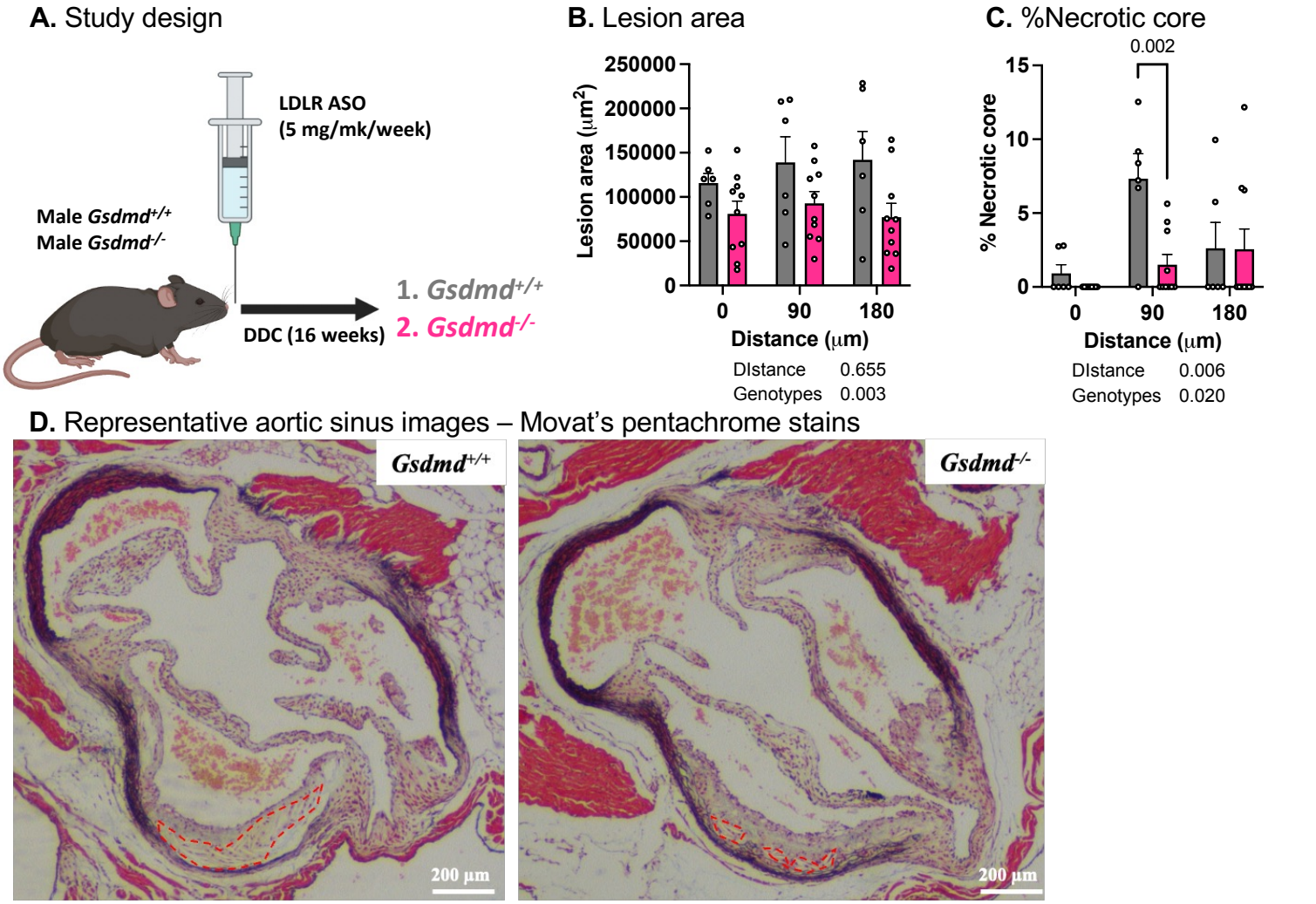

Supplemental Figure 1. Mice with whole-body gasdermin D deficiency demonstrate atheroprotective effects. For genotyping, blood and peritoneal cavity lavage were collected immediately following euthanasia. Leukocytes were enriched from the samples by removing erythrocytes with an ammonium-chloride-potassium buffer. Spleen was harvested immediately after perfusion with PBS and mechanically homogenized with an ammonium-chloride-potassium buffer to remove erythrocytes. Erythrocytes-free spleen cells were purified with an ultrapure CD11B positive selection kit (Miltenyi Biotec) following the manufacturer's instructions. After removing erythrocytes, samples were purified for DNA following the manufacturer's instructions (QIAGEN). DNA samples were quantified for *Gsdmd* wildtype and knockout mutant gene (one base pair thymine insertion) expression with the real-time PCR method. DNA samples were incubated with Taqman gene expression master mix (Thermo Fisher Scientific), *Gsdmd* forward primer (5'-GTCGATGGGAACATTCAG-3'), *Gsdmd* reverse primer (5'-TGAGTCACACGCAGTATA-3'), *Gsdmd* wildtype probe (5'-/56FAM/CCT+GA+C+A+AA+CA+TCA/3IABkFQ/-3'), and *Gsdmd* mutant probe (5'-/5HEX/CCT+GA+C+A+A+CA+TCA/3IABkFQ/-3; all from Integrated DNA Technologies). Initial denaturation at 95ºC, 10 minutes, cycling denaturation at 95ºC, 10 seconds, cycling annealing at 60ºC, 30 seconds, cycling extension at 72ºC, 10 seconds, 40 cycles. Male mice with and without gasdermin D-deficiency were maintained on a high-fat high-sucrose diet for 16 weeks to allow the formation of atherosclerotic lesions Mice received weekly i.p. injection of GalNAc-conjugated LDLR ASO (5 mg/kg) throughout the study. **A.** Schematic of study design. **B.** Aortic sinus lesion area. **C.** Aortic sinus % necrotic core calculated as necrotic core area/lesion area. **D.** Representative aortic sinus lesions stained with Movat's pentachrome stain. Representative necrotic core areas are circled in red. Data show means ± SEM (n=6, 10 mice/group). Statistical analyses were performed by two-way ANOVA (group effect p-values underneath graphs) followed by Tukey's multiple comparisons test (p-values indicated above bars). Outliers were removed based on Grubbs' test with alpha = 0.01. (0,1,0,0,0,0) data points were removed in C; no data points were removed in B.

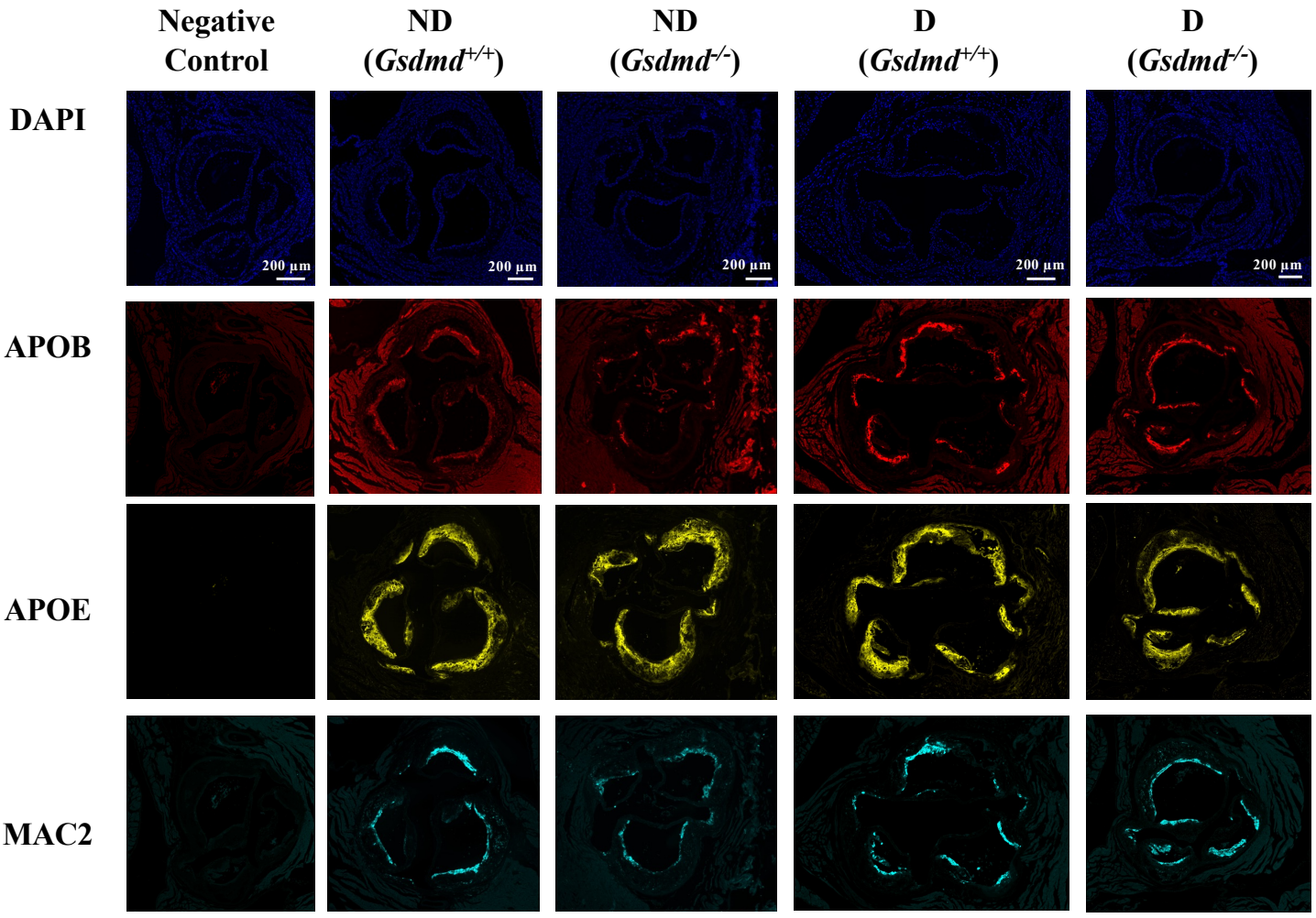

Supplemental Figure 2. Representative aortic sinus images from the type 1 diabetes-accelerated atherosclerosis mouse model with and without hematopoietic gasdermin D-deficiency stained for nuclei (DAPI), APOB, APOE, or MAC2. Female *Ldlr*$^{-/-}$*;Gp*^{Tg} mice were maintained on a high-fat diet (HFD) for 12 weeks to allow the formation of pre-existing lesions. Mice were lethally irradiated and received bone-marrow cells from animals with and without gasdermin D-deficiency. The animals were maintained on a chow diet and recovered for 5 weeks. Mice were rendered diabetic (D) with lymphocytic choriomeningitis virus (LCMV). Saline was used as a control (non-diabetic, ND). At the onset of diabetes, the animals were switched to a low-fat, semipurified diet with no added cholesterol (LFD) and were maintained for 4 weeks. Immunohistochemistry was performed using the antibodies and negative controls listed in Supplemental Table 2. Biotinylated goat IgG was used as the negative control for APOB. Rabbit IgG was used as the negative control for APOE. Rat IgG was used as the negative control for MAC2.

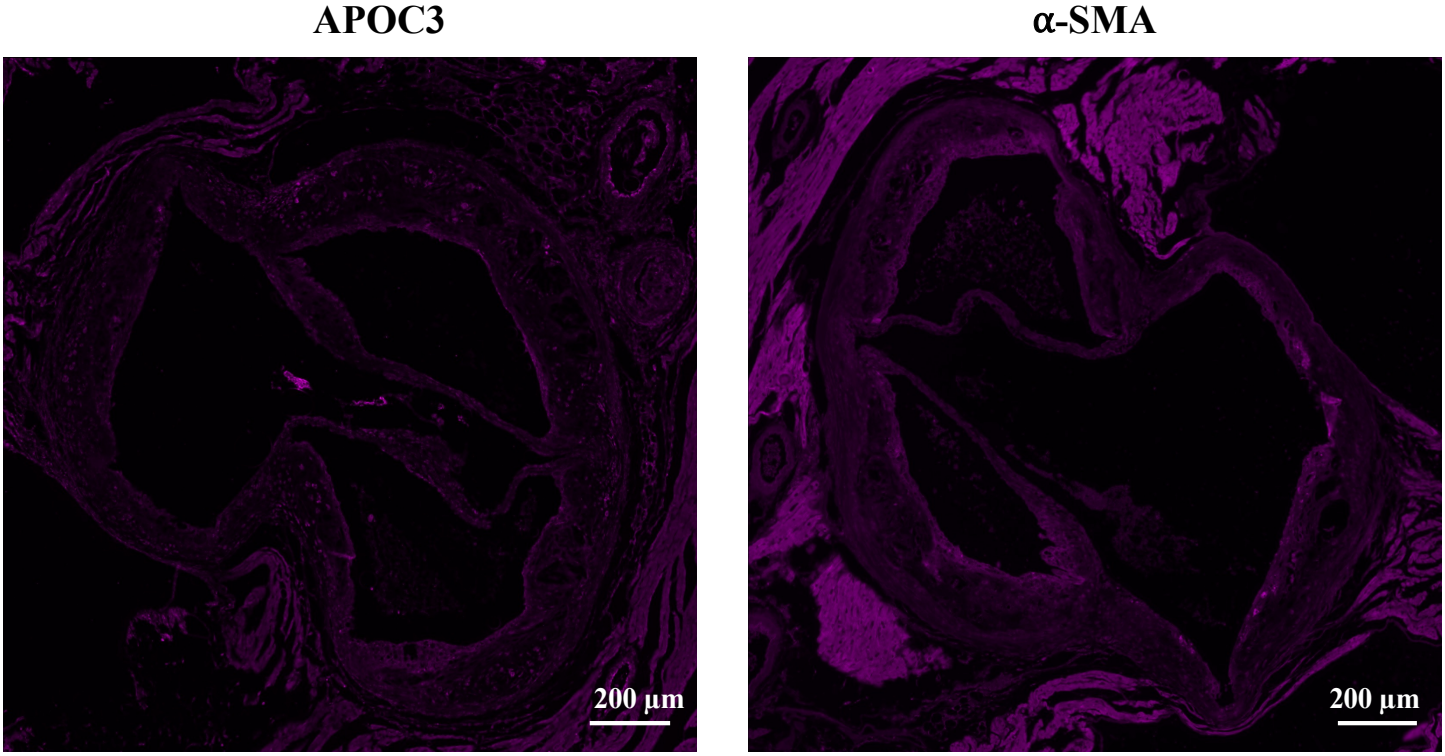

Supplemental Figure 3. Representative aortic sinus negative controls for APOC3 and α-SMA immunohistochemistry. Female *Ldlr*$^{-/-}$*;Gp*^{Tg} mice were maintained on a high-fat diet (HFD) for 12 weeks to allow the formation of pre-existing lesions. Mice were lethally irradiated and received bone-marrow cells from animals with and without gasdermin D-deficiency. The animals were maintained on a chow diet and recovered for 5 weeks. Mice were rendered diabetic (D) with lymphocytic choriomeningitis virus (LCMV). Saline was used as a control (non-diabetic, ND). At the onset of diabetes, the animals were switched to a low-fat, semipurified diet with no added cholesterol (LFD) and were maintained for 4 weeks. Immunohistochemistry was performed using the antibodies and negative controls listed in Supplemental Table 2. Normal rabbit serum was used as the negative control for APOC3. Rabbit IgG was used as the negative control for α-SMA.

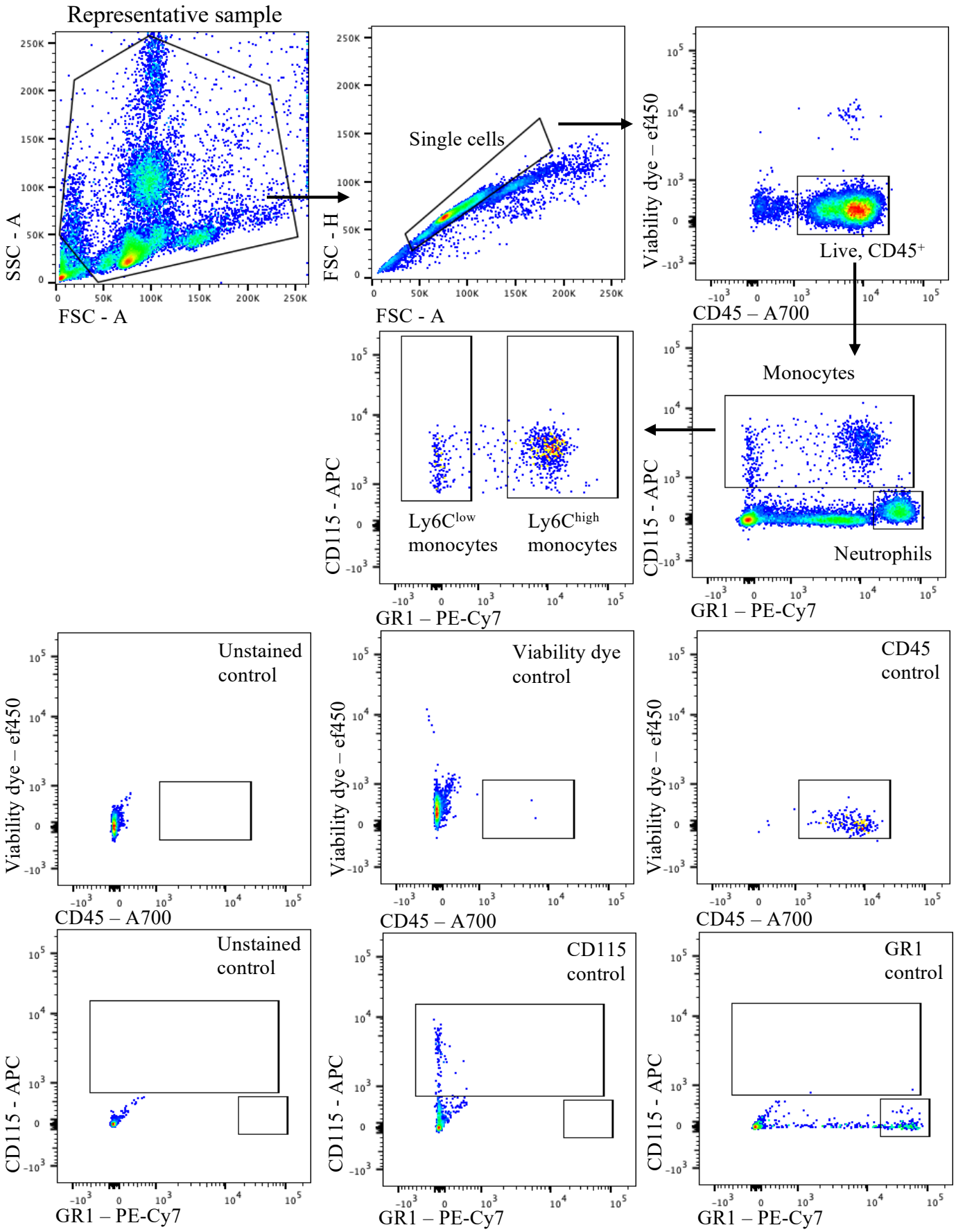

Supplemental Figure 4. Flow cytometry gating of blood samples. The gating strategy was determined with single-stained and unstained controls. Live, CD45$^+$ population (CD45$^+$, viability dye$^-$) was gated after gating for single cells. Monocytes (CD115$^+$) and neutrophils (CD115$^-$, GR1$^+$) were gated from the live, CD45$^+$ population. The monocyte population was further gated for ly6C^{high} (GR1$^+$) and ly6C^{low} (GR1$^-$) populations.

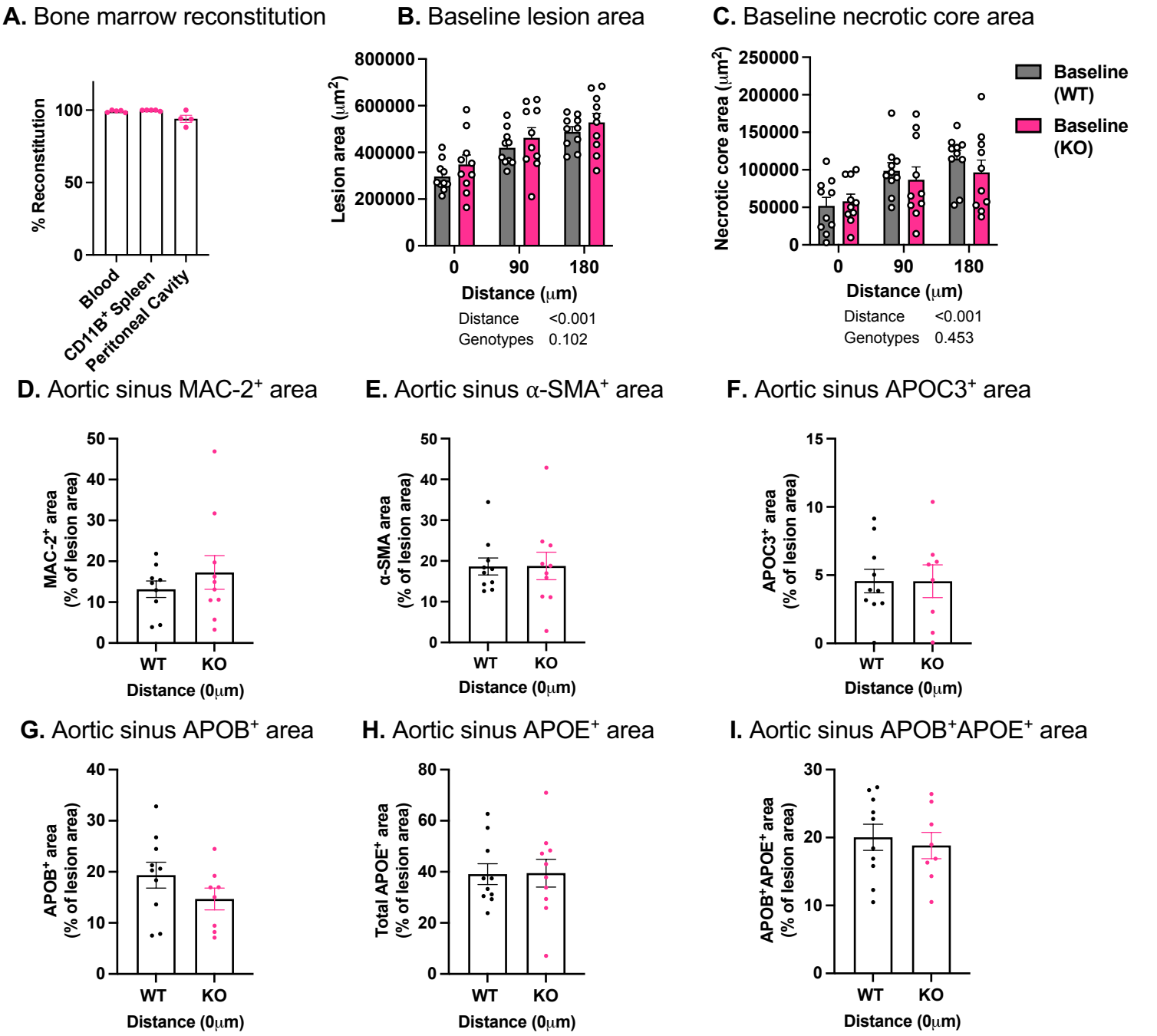

Supplemental Figure 5. Despite good reconstitution efficiency, mice with hematopoietic gasdermin D-deficiency show no differences in lesion morphologies at baseline. Female *Ldlr*$^{-/-}$;*Gp*^{Tg} mice were maintained on a high-fat diet (HFD) for 12 weeks to allow the formation of pre-existing lesions. Mice were lethally irradiated and received bone-marrow cells from animals with and without gasdermin D-deficiency. The animals were maintained on a chow diet and recovered for 5 weeks. Animals was euthanized after 5 weeks of recovery to evaluate lesion morphology before diabetes (baseline). **A.** % reconstitution of gasdermin D-deficiency donor cells in the blood, CD11B^{+} spleen, and peritoneal cavity cells harvested from the recipient mice. **B.** Aortic sinus lesion area. 0 μm represents the first appearance of the three aortic valve leaflets. **C.** Aortic sinus necrotic core area. **D.** Aortic sinus MAC2^{+} area. **E.** Aortic sinus α-SMA^{+} area. **F.** Aortic sinus APOC3^{+} area. **G.** Aortic sinus total APOB^{+} area. **H.** Aortic sinus total APOE^{+} area. **I.** Aortic sinus APOB^{+}APOE^{+} area. Immunofluorescence staining of MAC2, α-SMA, APOC3, APOB, and APOE were conducted at 0 μm. Data show means ± SEM (n=5, 5, 4 mice/group in A; n=10 mice/group in B-E; n=10, 9 mice/group in F; n= 10, 8 mice/group in G-I). Statistical analyses were performed by two-way ANOVA followed by Tukey's multiple comparisons test in B-C; Mann-Whitney test in D-E and G-H; Welch's test in F and I. Normality test was performed by D'Agostino & Pearson test. Outliers were removed based on Grubbs' test with alpha = 0.01. (1,0) data points were removed in D; (0,1) data points were removed in F; no data points were removed in A-C, E, and G-I.

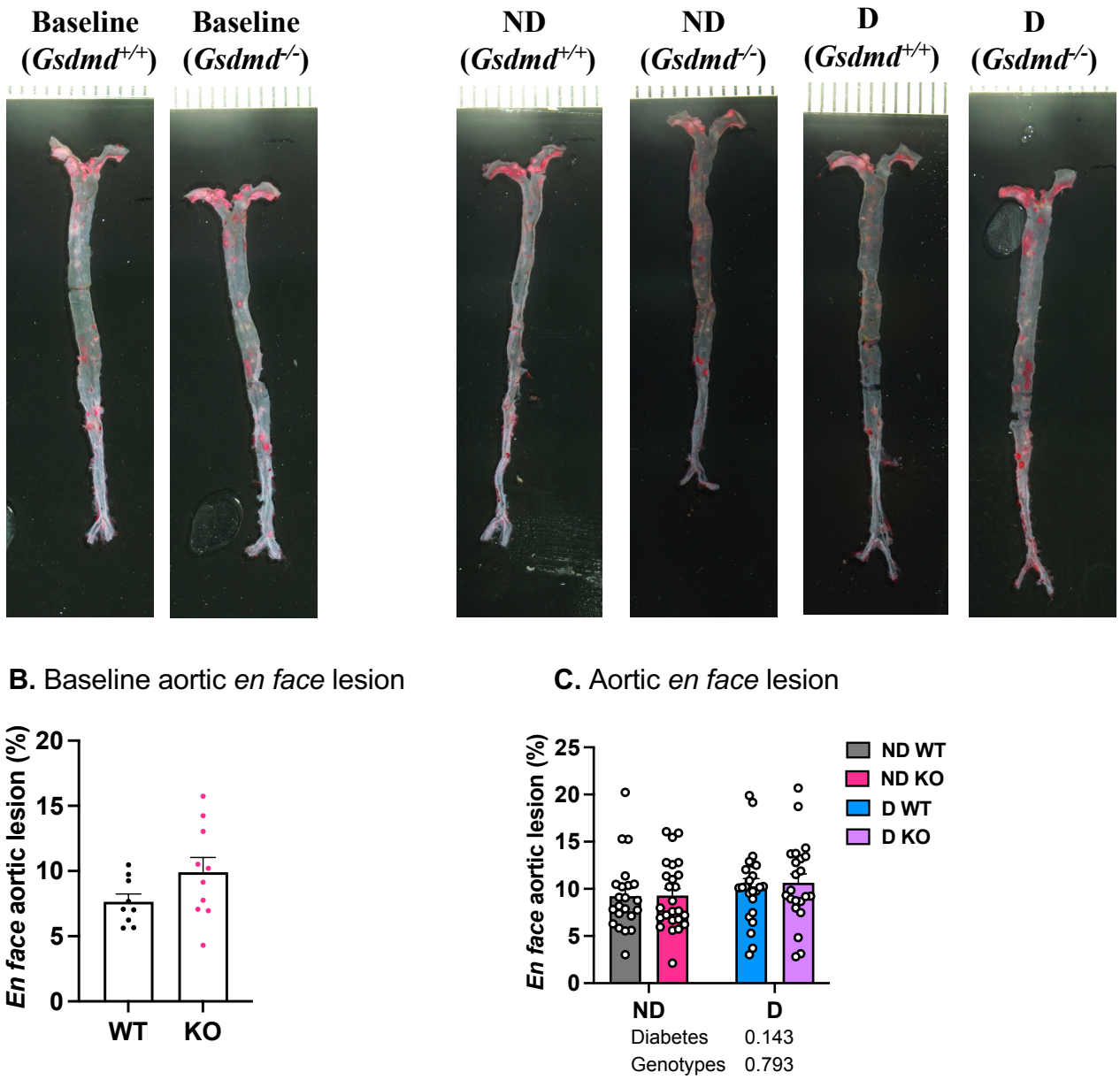

Supplemental Figure 6. Neither diabetes nor gasdermin D affects aortic Sudan IV-positive *en face* area in mice with pre-existing lesions. Female *Ldlr*$^{-/-}$*;Gp*^{Tg} mice were maintained on a high-fat diet (HFD) for 12 weeks to allow the formation of pre-existing lesions. Mice were lethally irradiated and received bone-marrow cells from animals with and without gasdermin D-deficiency. The animals were maintained on a chow diet and recovered for 5 weeks. Mice were rendered diabetic (D) with lymphocytic choriomeningitis virus (LCMV). Saline was used as a control (non-diabetic, ND). At the onset of diabetes, the animals were switched to a low-fat, semipurified diet with no added cholesterol (LFD) and were maintained for 4 weeks. A subset of animals was euthanized after 5 weeks of recovery to evaluate aortic Sudan IV-positive area before diabetes (baseline). **A.** Representative aortic *en face* lesions with Sudan IV staining. **B.** Aortic *en face* Sudan IV lesion at baseline. **C.** Aortic *en face* Sudan IV lesion. Data show means ± SEM (n=10 mice/group in B; n=22, 25, 24, 23 mice/group in C). Statistical analyses were performed by Welch's test in B; two-way ANOVA followed by Tukey's multiple comparisons test in C. Normality test was performed by D'Agostino & Pearson test. The text underneath panel C indicates group effects (p-values) as calculated by two-way ANOVA. Outliers were removed based on Grubbs' test with alpha = 0.01. (1,0) data points were removed in B; no data points were removed in C.

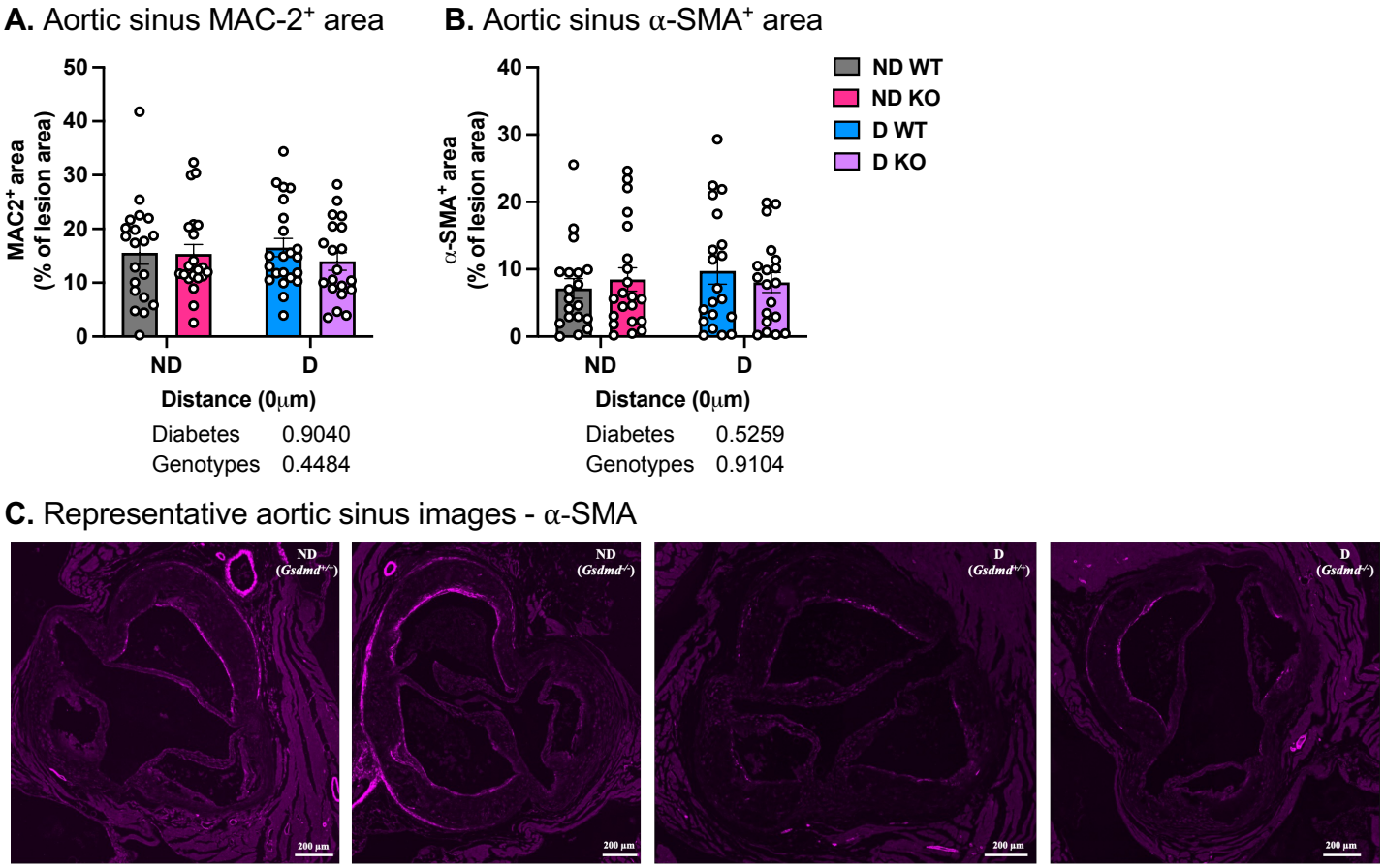

Supplemental Figure 7. Neither diabetes nor hematopoietic gasdermin D-deficiency alters macrophage or smooth muscle accumulation in pre-existing lesions of atherosclerosis. Female *Ldlr*$^{-/-}$*;Gp*^{Tg} mice were maintained on a high-fat diet (HFD) for 12 weeks to allow the formation of pre-existing lesions. Mice were lethally irradiated and received bone-marrow cells from animals with and without gasdermin D-deficiency. The animals were maintained on a chow diet and recovered for 5 weeks. Mice were rendered diabetic (D) with lymphocytic choriomeningitis virus (LCMV). Saline was used as a control (non-diabetic, ND). At the onset of diabetes, the animals were switched to a low-fat, semipurified diet with no added cholesterol (LFD) and were maintained for 4 weeks. **A.** Aortic sinus MAC2^{+} area. **B.** Aortic sinus α-SMA^{+} area. **C.** Representative aortic sinuses stained with an α-SMA antibody. Immunofluorescence staining of MAC2 and α-SMA were conducted at 0 μm. Data show means ± SEM (n=20, 22, 21, 20 mice/group in A; n=19, 21, 20, 19 mice/group in B). Statistical analyses were performed by two-way ANOVA (group effect p-values underneath graphs). Outliers were removed based on Grubbs' test with alpha = 0.01. No data points were removed in A-B.

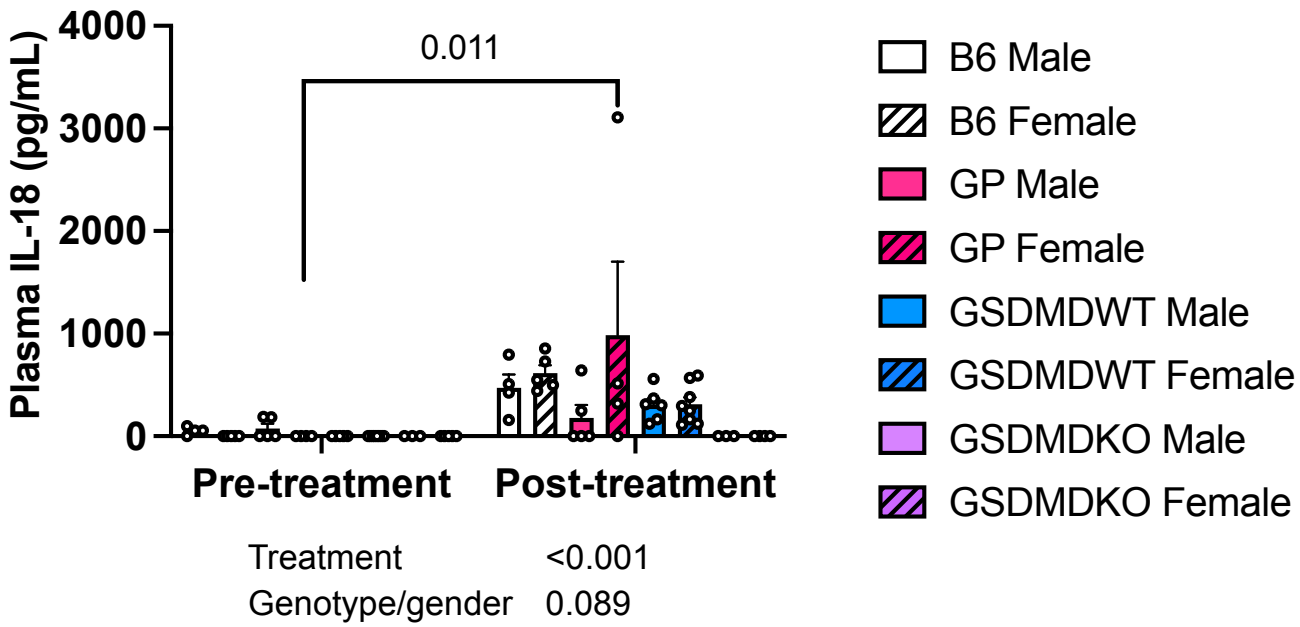

Supplemental Figure 8. Neither gender nor genotype affects the release of IL-18 to plasma. Male and female mice with and without whole-body gasdermin D (GSDMD)-deficiency and with and without transgenic glycoprotein (GP) received i.p. injections with and without ultrapure LPS and ATP to induce inflammasome activation. Data show means ± SEM (n=4-8 individual mice/group). Statistical analyses were performed by two-way ANOVA (group effect p-values underneath graphs) followed by Tukey's multiple comparisons test (p-values indicated above bars). Outliers were removed based on Grubbs' test with alpha = 0.01. (0,0,0,1,1,0,1,0; 0,0,0,1,0,0,1,1) data points were removed. B6, C57BL/6 mice; GP, *Ldlr*$^{-/-}$ *Gp*^{Tg} mice; GSDMDWT, C57BL/6 wildtype GSDMD controls; GSDMDKO, C57BL/6 whole-body GSDMD-deficient mice.

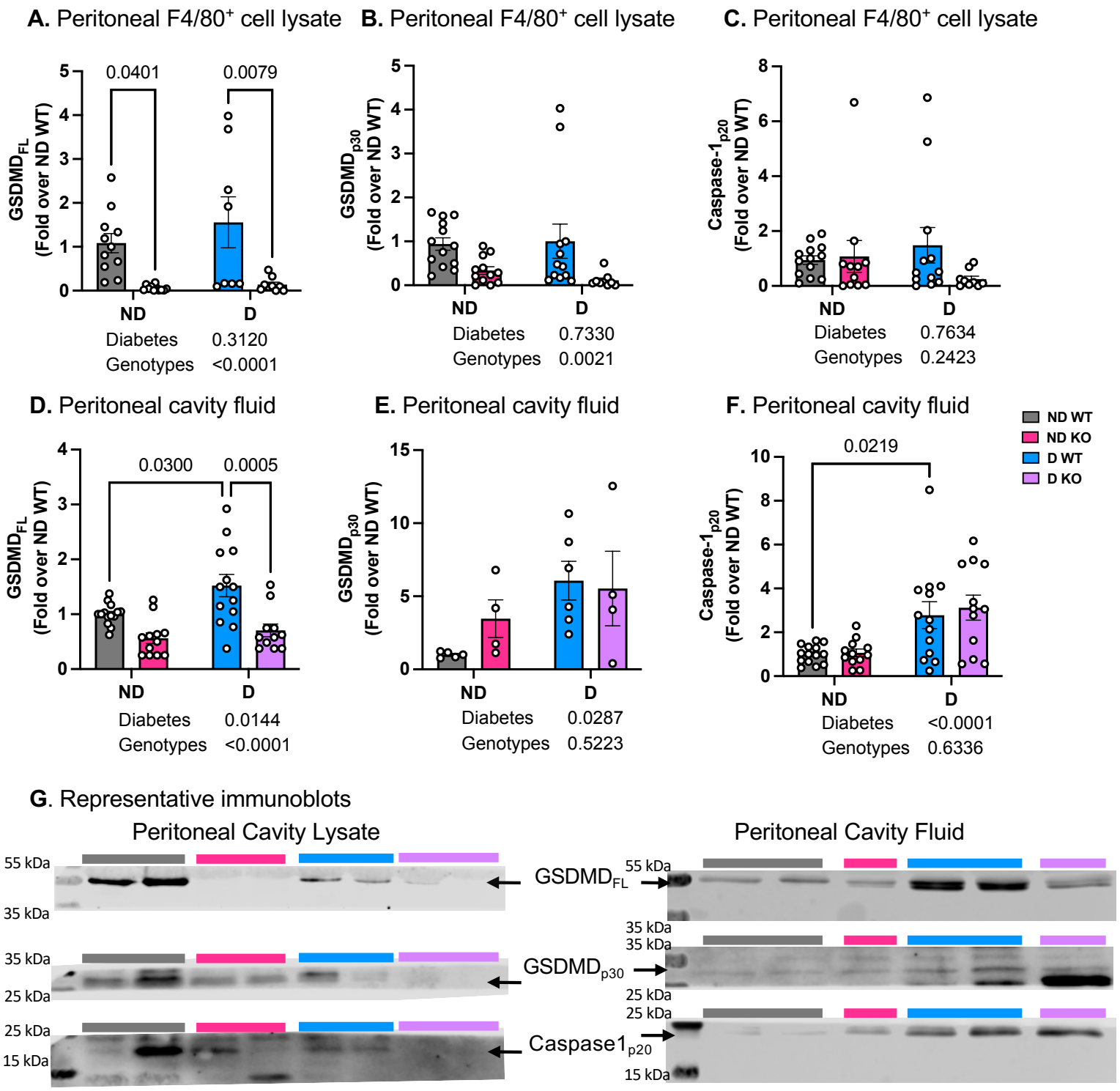

Supplemental Figure 9. Diabetes induces inflammasome activation in F4/80- cells in the peritoneal cavity through a mechanism independent of hematopoietic GSDMD-deficiency. Peritoneal cavity fluid and cells were isolated from the lavage with centrifugation from the mice described in figure 2. Peritoneal cavity cells were further enriched with F4/80-positive immunoselection beads. Peritoneal cavity F4/80+ cell lysate was immunoblotted for **A.** Full-length gasdermin D. **B.** Cleaved gasdermin D. **C.** Cleaved caspase1. Peritoneal cavity fluid was immunoblotted for **D.** Full-length gasdermin D. **E.** Cleaved gasdermin D. **F.** Cleaved caspase1. **G.** Representative immunoblots. Data show means ± SEM (n=11, 11, 8, 9 mice/group in A; n=13, 12, 12, 10 mice/group in B; n=13, 12, 12, 9 mice/group in C; n=14, 12, 13, 12 mice/group in D and F; n=5, 4, 6, 4 mice/group in E). Statistical analyses were performed by two-way ANOVA (group effect p-values underneath graphs) followed by Tukey's multiple comparisons test (p-values indicated above bars) in A-F. Outliers were removed based on Grubbs' test with alpha = 0.01. (0,0,0,1) data points were removed in B; (0,1,0,0) data points were removed in C; (0,0,0,1) data points were removed in D; no data points were removed in A and E-F.

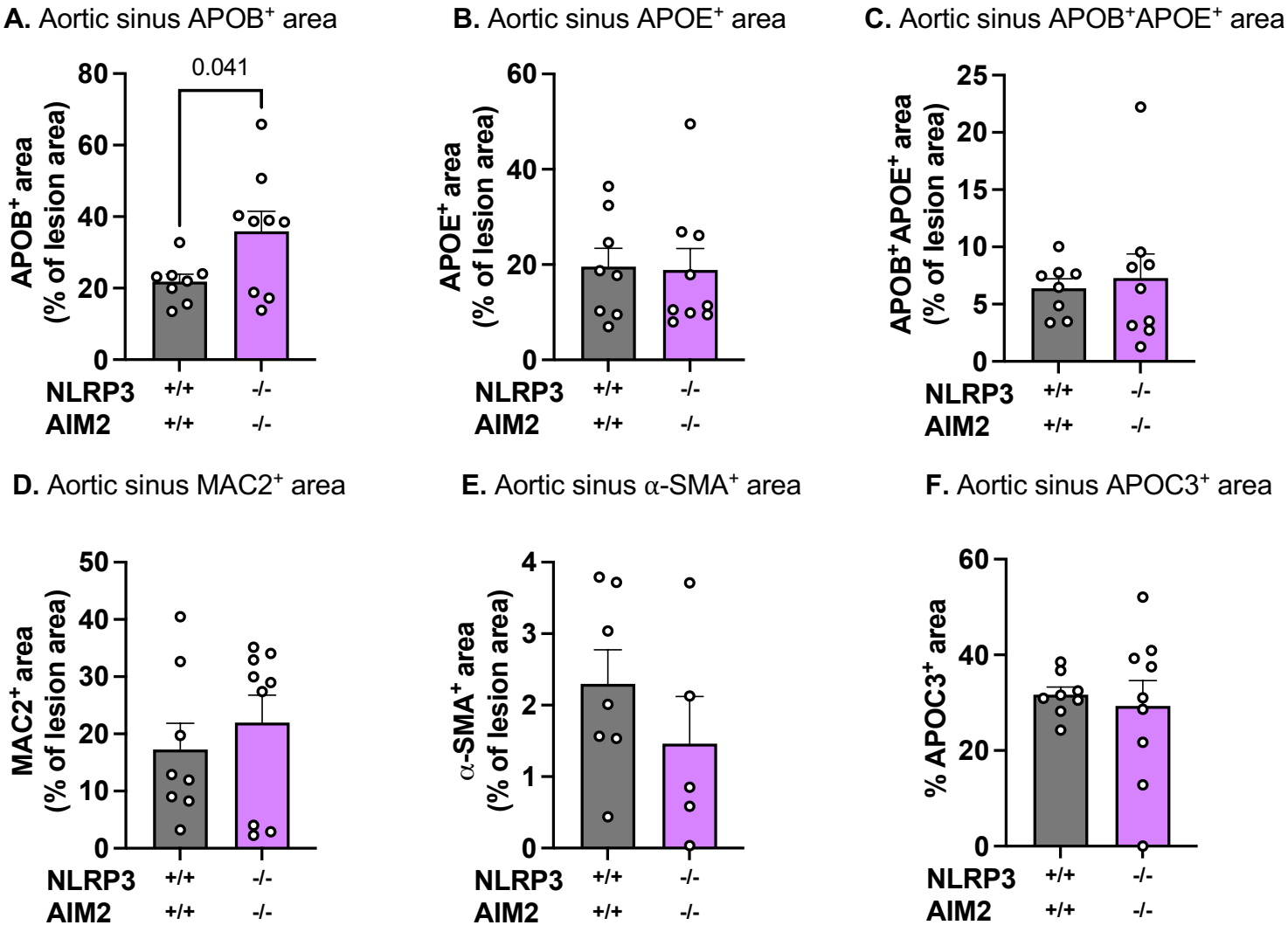

Supplemental Figure 10. Hematopoietic AIM2-, NLRP3-, and AIM2/NLRP3 double-deficiencies contribute to lesion area but not necrotic core area in the setting of diabetes. Female *Ldlr*$^{-/-}$ mice were lethally irradiated and received bone-marrow from mice with and without NLRP3-deficiency (*Nlrp3*$^{-/-}$), AIM2-deficiency (*Aim2*$^{-/-}$), or double-deficiency of NLRP3 and AIM2 (DKO). The animals were recovered on chow for 4 weeks before diabetes was induced with 5 days of streptozotocin (STZ) injections (50 mg/kg/day). Animals were maintained on a Western diet for 8 weeks. **A.** Aortic sinus APOB^{+} area expressed as % of lesion area (total APOB^{+} area; 68,408±12,054 v.s. 67,017±12,116 μm^2; NLRP3$^{+/+}$AIM2$^{+/+}$ v.s. NLRP3$^{-/-}$AIM2$^{-/-}$; p=0.936). **B.** Aortic sinus APOE^{+} area expressed as % of lesion area (total APOE^{+} area; 61,686±12,358 v.s. 34,583±8,040 μm^2; p=0.09). **C**. Aortic sinus APOB^{+}APOE^{+} area expressed as % of lesion area (total APOB^{+}APOE^{+} area; 21,750±4,847 v.s. 14,865±5,147 μm^2; p=0.236). **D.** Aortic sinus MAC2^{+} area expressed as % of lesion area (total MAC2^{+} area; 41,156±6,787 v.s. 40,113±8,620 μm2, p=0.926). **E.** Aortic sinus α-SMA^{+} area expressed as % of lesion area (total α-SMA^{+} area; 8,062±2,921 v.s. 3,610±1,876 μm^2; p=0.202). **F.** Aortic sinus APOC3^{+} area expressed as % of lesion area (total APOC3^{+} area; 5,187±1,080 v.s. 2,589±821 μm^2; p=0.128). Data show means ± SEM (n= 5-9 mice/group). Statistical analyses were performed by Welch's t test in A, D, and F; Mann-Whitney test in B, C, and E. Normality test was performed by D'Agostino & Pearson test. Outliers were removed based on Grubbs' test with alpha = 0.01. No data points were removed in A-F.

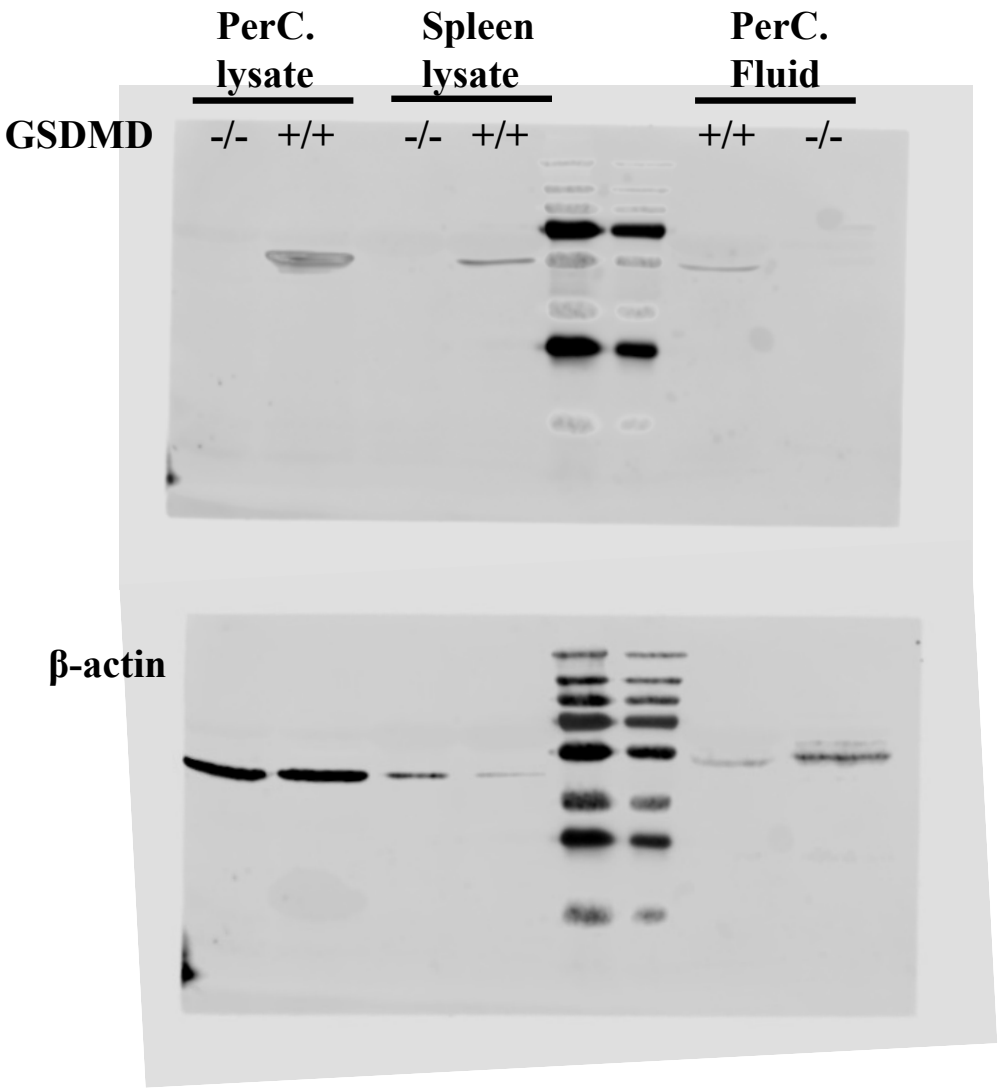

Supplemental Figure 11. Immunoblotting of gasdermin D (GSDMD) and β-actin from animals with and without gasdermin D-deficiency. Peritoneal cavity fluid, cell lysate, and spleen cell lysate were harvested from mice with and without gasdermin D-deficiency.

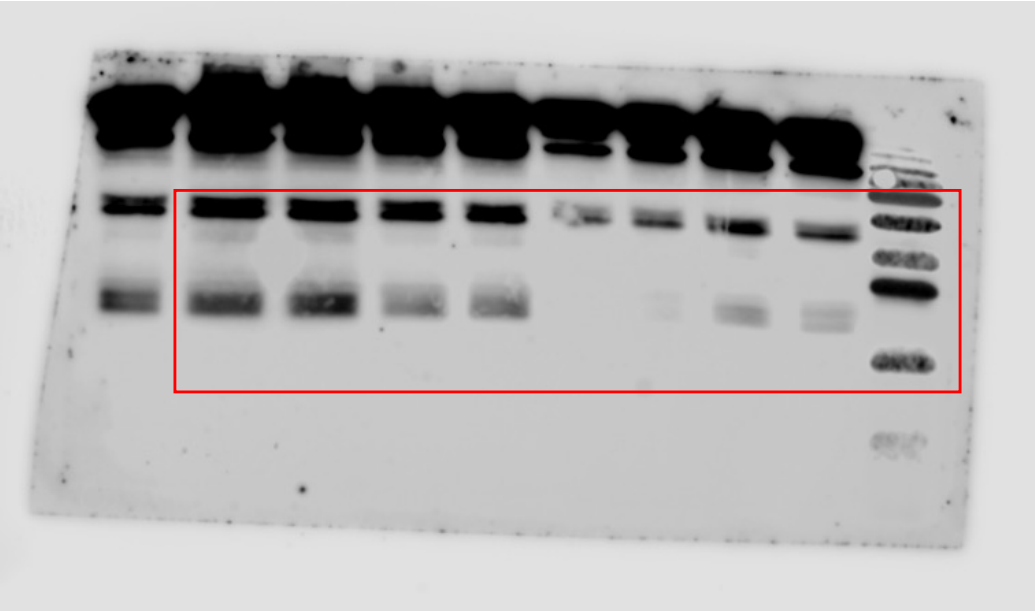

Supplemental Figure 12. Immunoblot of cropped blot used in figure 1I. The section cropped is boxed in red.

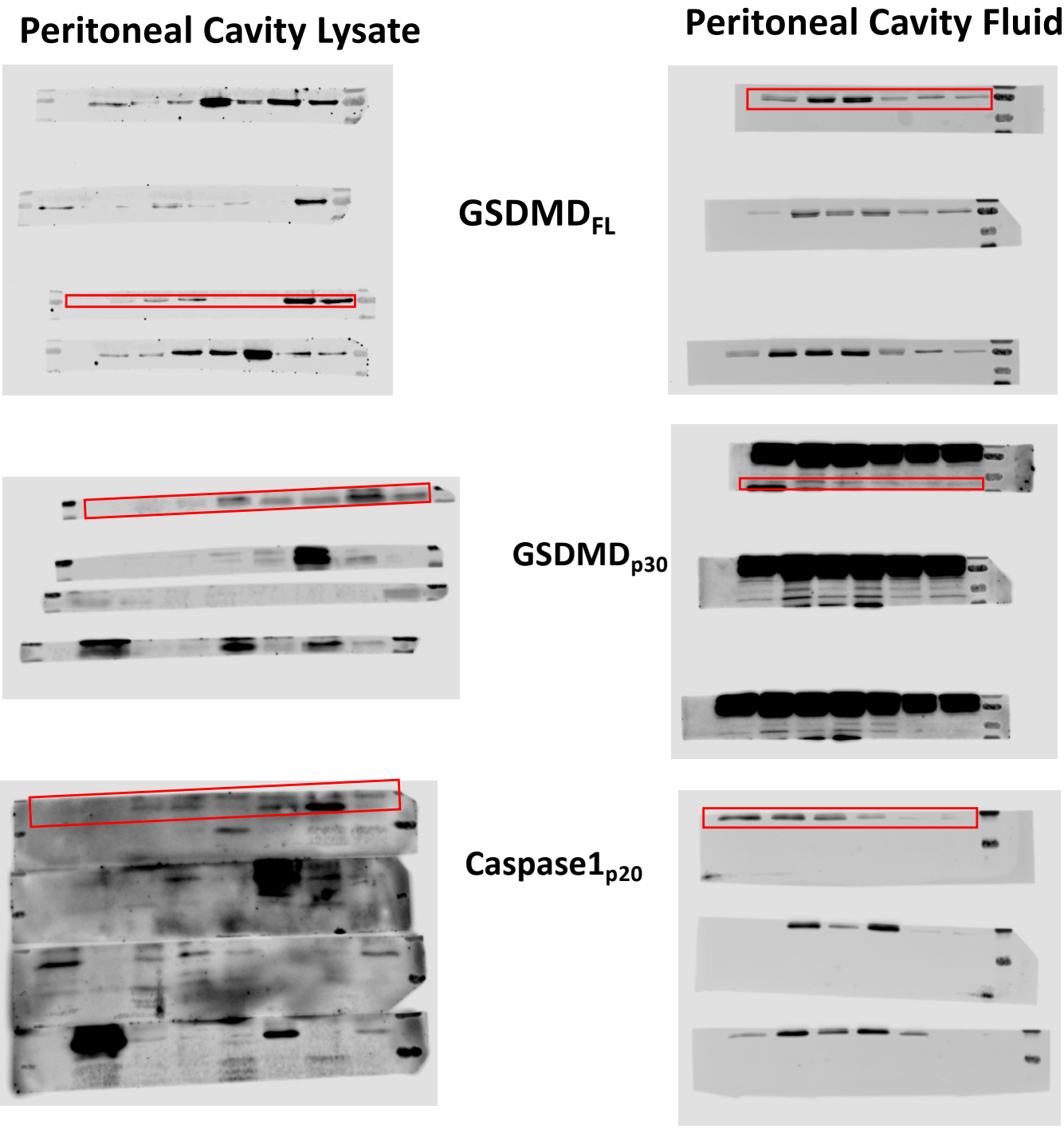

Supplemental Figure 13. Immunoblots of cropped blots used in supplemental figure 7G. The section cropped are boxed in red.

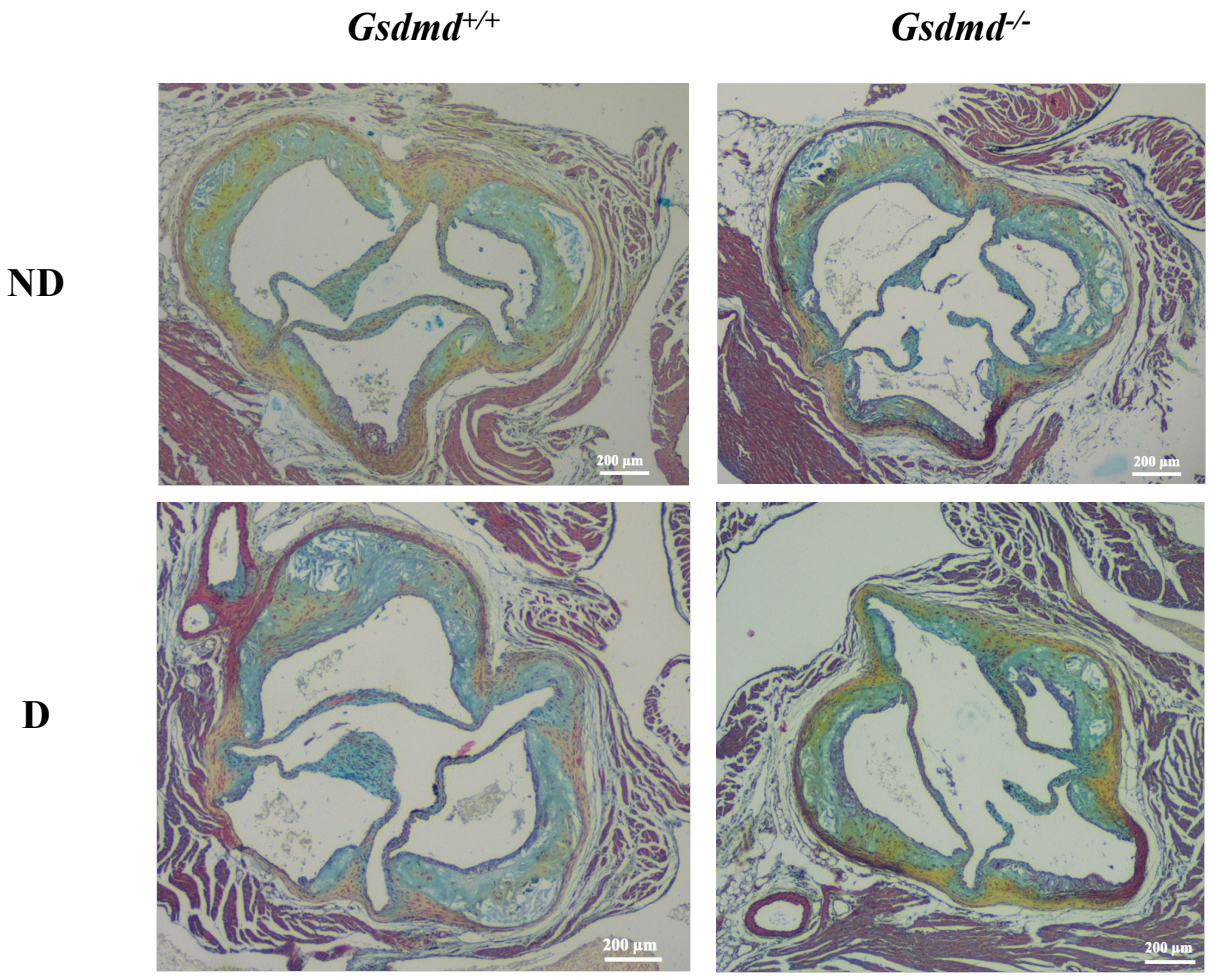

Supplemental Figure 14. Unmarked aortic lesion images used in figure 2J.